Multiscale Crowd Dynamics Modeling and Theory

Andrea Tosin*

* Istituto per le Applicazioni del Calcolo "M. Picone"
Consiglio Nazionale delle Ricerche, Rome, Italy

Abstract This chapter deals with models of living complex systems, chiefly human crowds, by methods of conservation laws and measure theory. We introduce a modeling framework which enables one to address both discrete and continuous dynamical systems in a unified manner using common phenomenological ideas and mathematical tools as well as to couple these two descriptions in a multiscale perspective. Furthermore, we present a basic theory of well-posedness and numerical approximation of initial-value problems and we discuss its implications on mathematical modeling.

1 Introduction

By *living complex systems* we mean multi-agent systems composed by living entities, which take part in *group dynamics* while trying to chase *individual purposes*. Specifically, in this chapter we will be concerned with human crowds. We will assimilate pedestrians to *active particles*, the *activity* being their ability to set one or more intermediate and final goals (such as e.g, avoiding collisions with other particles, reaching a destination) and to act directly on their own dynamics to chase them, without being passively prone to external influences. This gives rise to *collective* dynamics based primarily on *individual* behavioral rules. At times active particles cooperate for chasing a group goal, like in *consensus* and *rendez-vous* problems studied by Canuto et al. (2012). On other occasions, instead, they do not cooperate consciously, which makes group dynamics more difficult to be predicted and nevertheless often surprisingly ordered and coordinated: it is the so-called *self-organization*, see Cristiani et al. (2010).

In order to model such systems it is necessary to set up mathematical structures suitable to cope with their complexity, partly due to that overall dynamics are ultimately *multiscale*. In fact, they originate from individual

A. Muntean, F. Toschi (Eds.), *Collective Dynamics from Bacteria to Crowds*, CISM International Centre for Mechanical Sciences, DOI 10.1007/978-3-7091-1785-9_6,

behaviors at the *microscopic* scale of single particles. Next, they are "amplified" by interactions among particles up to producing collective behaviors at the *macroscopic* scale of the group, which cannot be directly deduced from the knowledge of individual ones. Moreover, the collective state of the group can in turn impact locally on the behavioral rules adopted by single particles.

A large class of mathematical models uses *conservation* (or *balance*) *laws*, expressing the fact that some physical quantities, such as mass, linear momentum, and energy of the system, either do not change during the evolution or change in consequence of specific production/destruction mechanisms. However, living systems can hardly be confined in strict balance principles. For instance, their ability to elaborate *behavioral strategies* for chasing a purpose makes them continuously put and remove energy from the system in unconventional manners. Indeed entropy principles classically related to the equiprobability of the states may be questioned, for self-organization promotes special, usually inhomogeneous, configurations to the detriment of more generic and homogeneous ones as stated by Schröedinger (1967). Moreover, it may be difficult to ascribe the variations of linear momentum to possibly "generalized" forces, because the dynamics of living systems are not ruled purely by inertia. Of course, active particles do not elude usual physical laws, rather they can influence them by means of personal decisions, whose effects are not necessarily describable in terms of external force fields. In other words, a straightforward application of the very same ideas successfully used to describe other kinds of passive systems may not completely fit active particles, because this analogy would forcedly miss some distinctive features that heavily differentiate living from inert matter.

Among all classical balance principles mentioned above, probably the less questionable one for the systems at hand is the conservation of mass: when describing the evolution in space and time of human crowds it makes sense to assume that no proliferation or destruction of pedestrians occur. Notice that this does not imply by itself any specific dynamics of the interactions among the individuals, it simply requires the conservation of their number. Thus interactions can still be mechanical or non-mechanical, local or nonlocal, binary or multiple, and so on.

Starting from the mass conservation principle, in this chapter we describe a unified mathematical framework which allows one to model crowd dynamics by embedding the discrete description of individual pedestrians and the continuous one of the collectivity. The key point is the reinterpretation of the continuity equation in terms of abstract mass measures featuring a singular component (Dirac deltas), which represents the discrete level, and an absolutely continuous one (with respect to the Lebesgue measure), which

represents the continuous level. In more detail, in Section 2 we first introduce the abstract equation and then specialize it to the case of pedestrian interaction models. In Section 3 we discuss the use of the measure formulation for obtaining discrete, continuous, and multiscale models, relating furthermore the structure of the measure and the behavioral strategy of pedestrians. In Section 4 we present the basic qualitative results concerning well-posedness and numerical approximation of the Cauchy problem for the mathematical structures previously deduced. Finally, in Section 5 we discuss the relevance of these qualitative results as guidelines for the construction of specific models which are both physically realistic and mathematically robust.

2 Mathematical models by time-evolving measures

From the mathematical point of view, the *mass* of a d-dimensional system ($d = 1, 2, 3$ for physical purposes) at time t is a Radon positive measure $\mu_t : \mathcal{B}(\mathbb{R}^d) \to \mathbb{R}_+$ defined over the Borel σ-algebra $\mathcal{B}(\mathbb{R}^d)$ in the physical space $\mathbb{R}^d$. In our case, for all measurable set $E \in \mathcal{B}(\mathbb{R}^d)$ the number $\mu_t(E) \geq 0$ gives an estimate of the crowding of the region $E \subseteq \mathbb{R}^d$ at time t (ideally, it can be thought of as the "average" number of pedestrians occupying the region E at time t). In particular, if we consider a crowd composed by N pedestrians then, owing to the mass conservation principle, we must have $\mu_t(\mathbb{R}^d) = N$ for all t. This can be expressed in differential form by saying that the measure μ_t satisfies the equation:

$$\frac{\partial \mu_t}{\partial t} + \nabla \cdot (\mu_t v_t) = 0, \tag{1}$$

where $v_t = v_t(x) : \mathbb{R}^d \to \mathbb{R}^d$ is, at time t, a transport velocity field. Equation (1) is written in a formal fashion but has to be properly understood in the weak sense of distributions. For all test function $\phi \in C_c^\infty(\mathbb{R}^d)$ and for all $t \in (0, T_{\max}]$, $T_{\max} > 0$ being a final time, it means:

$$\int_{\mathbb{R}^d} \phi(x)\, d\mu_t(x) = \int_{\mathbb{R}^d} \phi(x)\, d\mu_0(x) + \int_0^t \int_{\mathbb{R}^d} v_s(x) \cdot \nabla \phi(x)\, d\mu_s(x)\, ds, \tag{2}$$

where μ_0 is a positive Radon measure to be assigned, which represents the initial distribution of the crowd. If the transport velocity is bounded, i.e., there exists a constant $V_{\max} > 0$ such that

$$|v_t(x)| \leq V_{\max}, \qquad \forall\, x \in \mathbb{R}^d,\ t \in (0, T_{\max}],$$

it is not difficult to show that (2) implies indeed $\mu_t(\mathbb{R}^d) = \mu_0(\mathbb{R}^d)$ for all $t \in (0, T_{\max}]$, hence actually the conservation of the total number of pedestrians

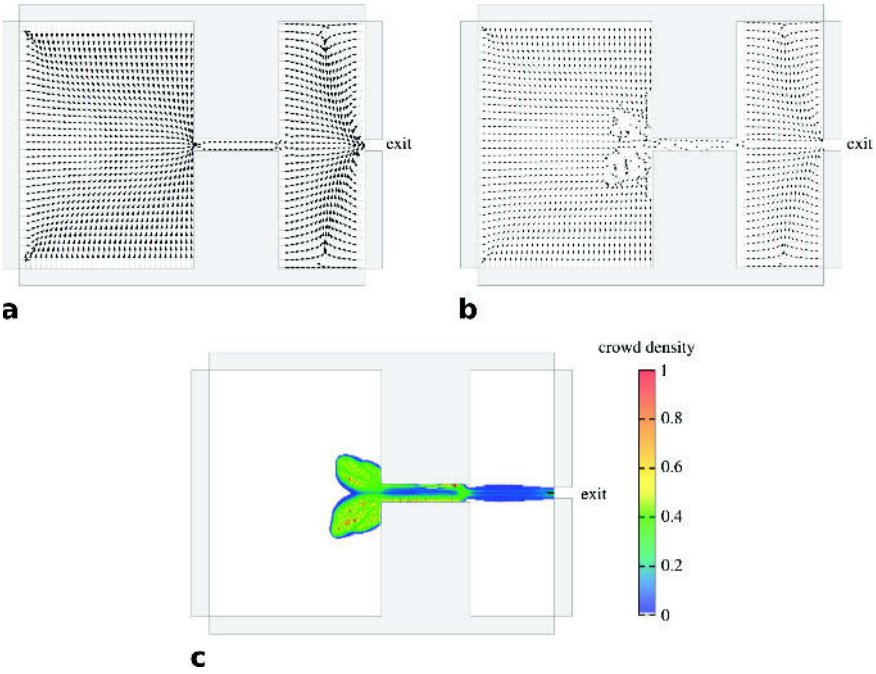

Figure 1. a. Example of a desired velocity field v_d in a domain formed by two regions communicating through a narrow corridor. **b.** "True" velocity v (cf. Equation (3)) when the interaction velocity v_i among pedestrians is added to the desired velocity. **c.** Crowd density field with generates the true velocity illustrated in **b.**

as fixed at the initial time. It is sufficient to take a sequence $\{\phi_m\}_{m\geq 1} \subseteq C_c^\infty(\mathbb{R}^d)$ of test functions such that $0 \leq \phi_m(x) \leq 1$ for all $x \in \mathbb{R}^d$ and all $m \geq 1$, with in addition $\phi_m(x) \to 1$ and $\nabla\phi_m(x) \to 0$ pointwise for $m \to \infty$, and then invoke the Dominated Convergence Theorem (the existence of such a sequence is guaranteed by Uryshon's Lemma).

2.1 Modeling pedestrian interactions

Equation (1), or alternatively (2), gives the time evolution of the crowd distribution μ_t provided a transport velocity is assigned. Recalling the discussion set forth in the Introduction, given the lack of a balance of linear momentum to be coupled to the mass conservation it is necessary to model directly the field v_t.

Other crowd models available in the literature follow similar ideas, see e.g., Coscia and Canavesio (2008); Colombo and Rosini (2009). Typically, pedestrian velocity is obtained from an empirical constitutive relationship, the so-called *fundamental diagram*, which expresses it as a known function of the distribution in space of the crowd in (locally) stationary homogeneous conditions. Here we propose instead a modeling of v_t more focused on pedestrian interactions, in order to ground the dynamics directly on the idea of active behavior discussed in the Introduction.

We write the velocity as the sum of two contributions:

$$v_t(x) := v_{\mathrm{d}}(x) + v_{\mathrm{i}}[\mu_t](x), \tag{3}$$

where square brackets indicate a functional dependence on the measure μ_t.

The function $v_{\mathrm{d}} : \mathbb{R}^d \to \mathbb{R}^d$ is the *desired velocity*, i.e., the velocity at which an isolated pedestrian would head for her destination. It is independent of the system dynamics, being determined *a priori* only by the geometry of the domain, including the presence of possible obstacles viewed as holes in $\mathbb{R}^d$, namely regions that pedestrian cannot access (Figure 1a). Conversely, the function $v_{\mathrm{i}}[\mu_t] : \mathbb{R}^d \to \mathbb{R}^d$ is the *interaction velocity*, i.e., the correction that pedestrians make to the desired velocity due to mutual interactions. It takes into account that individuals generally aim at avoiding crowded areas, hence it adds a *repulsive* contribution to v_{d} (Figures 1b-c). Moreover, its effect is *nonlocal*, because pedestrians anticipate their own decisions through a process of synthesis of the information about the crowd distribution in the immediate vicinity. Out of these arguments, we set:

$$v_{\mathrm{i}}[\mu_t](x) = \int_{\mathbb{R}^d} K(x,\, y)\eta_{\mathcal{S}(x)}(y)\, d\mu_t(y), \tag{4}$$

where:

- $K : \mathbb{R}^d \times \mathbb{R}^d \to \mathbb{R}^d$ is the *interaction kernel*, which describes the repulsion acting on the individual in x, called *test pedestrian*, because of the presence of an individual in y, called *field pedestrian*. Generally, recalling also the Galileian invariance, the function K depends on x, y through their distance $|y - x|$ along the segment connecting them. A prototypical example is:

$$K(x,\, y) \sim -\frac{1}{|y-x|} \cdot \frac{y-x}{|y-x|}$$

for $|y - x|$ "not too" small, whereas for $y \to x$ it may be necessary to introduce a regularization in order to avoid singularities (cf. Section 5);

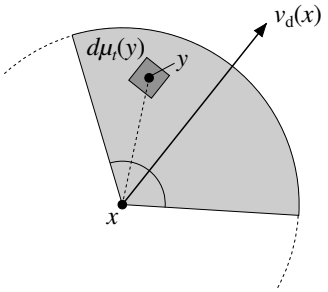

Figure 2. Sensory region of the test pedestrian in x.

- $\eta_{\mathcal{S}(x)} : \mathbb{R}^d \to \mathbb{R}_+$ is a *cut-off function* limiting the influence on the test pedestrian in x to field pedestrians within her *sensory region* $\mathcal{S}(x) \subset \mathbb{R}^d$. Typically, $\eta_{\mathcal{S}(x)}$ is smooth and compactly supported in $\mathcal{S}(x)$ (for instance, it can be a mollified version of the characteristic function of the set $\mathcal{S}(x)$). A prototypical sensory region is a circular sector centered in x, symmetric with respect to the local direction of the desired velocity $v_d(x)$, and oriented along the latter (Figure 2). This models *anisotropic* interactions: the test pedestrian is affected by field pedestrians ahead but not behind. The radius of the circular sector is the maximal distance at which a field pedestrian can have an influence on the test pedestrian, while the angle of the sector identifies the visual cone of the latter.

3 Multiscale approach

Equations (1), (3), (4) provide a unified modeling framework which comprises both *discrete* and *continuous* dynamics. The key point is the *spatial structure* of the measure μ_t.

Discrete dynamics are obtained if the spatial structure of μ_t is discrete:

$$\mu_t = \sum_{i=1}^{N} \delta_{x_i(t)}, \tag{5}$$

$\{x_i(t)\}_{i=1}^N \subset \mathbb{R}^d$ being the set of all and only points where pedestrians are distributed at time t. Plugging (5) into (2), (4) yields:

$$\dot{x}_i = v_d(x_i) + \sum_{j=1}^{N} K(x_i, x_j)\eta_{\mathcal{S}(x_i)}(x_j) \qquad (i = 1, \ldots, N), \tag{6}$$

which completely characterizes the evolution of the crowd distribution.

Continuous dynamics are instead obtained if the spatial structure of μ_t is continuous, i.e., if mass and volume are proportional (in the sense of Radon-Nikodym's Theorem):

$$d\mu_t(x) = \rho_t(x)\, dx, \tag{7}$$

where now $\rho_t : \mathbb{R}^d \to \mathbb{R}_+$ is the *mass density* of the crowd distribution at time t, such that $\int_{\mathbb{R}^d} \rho_t(x)\, dx = N$ (thus, in particular, $\rho_t \in L^1(\mathbb{R}^d)$ for all t). In this frame, the support of ρ_t in $\mathbb{R}^d$ is conceptually the counterpart of the set $\{x_i(t)\}_{i=1}^N$ above. Inserting (7) in (2), (4) gives (actually a weak form of):

$$\frac{\partial}{\partial t}\rho_t(x) + \nabla \cdot \left[\rho_t(x)\left(v_{\mathrm{d}}(x) + \int_{\mathbb{R}^d} K(x, y)\eta_{\mathcal{S}(x)}(y)\rho_t(y)\, dy\right)\right] = 0, \tag{8}$$

namely a conservation law with nonlocal flux, which in turn characterizes completely the evolution of the distribution of pedestrians.

Do Equations (6), (8) describe the same system and the same dynamics? Yes and no. They formalize two different mathematical models of the same physical system, which however originate from the common abstract structure (1)–(4). Therefore they share the phenomenological description of the *individual microscopic interactions*, expressed by the kernel K and by the cut-off function $\eta_{\mathcal{S}(\cdot)}$, but can predict different *collective macroscopic effects* because the latter depend on the spatial structure of the measure μ_t in Equation (4).

More precisely, it is useful to understand the spatial structure of μ_t as the modeling counterpart of the *perception* of the test pedestrian, which affects the way the latter reacts to surrounding individuals. A discrete perception can be typical of sparse crowds or of leisure-type travel purposes, when pedestrians are more sensitive to the *one-by-one* distribution of their neighbors. Conversely, a continuous perception can be typical of dense crowds or of business-type travel purposes (e.g., commuters in rush hours), when pedestrians tend to interact with *subgroups* of other walkers as a whole. This corresponds to the expression of a *behavioral strategy*, which can impact in a non-negligible manner on the classical laws of motion (see also Bruno et al. (2011) for a different modeling approach to the concept of perception, however always related to the expression of a behavioral strategy by pedestrians). Therefore, although the elementary pairwise interaction rules are always the same, their collective effect can be greatly different due to the "filtering" operated by perception. Such a phenomenology is possible because crowds are *granular living* systems: the number of

pedestrians is locally always finite and "small" (at least compared to the order of magnitude of the Avogadro's number in classical gas dynamics), which makes large-scale dynamics rather sensitive to individual behaviors on smaller scales.

The concept of perception can be formalized in the model by means of a parameter $\theta \in [0, 1]$, which determines a *scale* of spatial structures of the measure μ_t:

$$\mu_t = \theta \sum_{j=1}^{N} \delta_{x_j(t)} + (1-\theta)\rho_t \mathcal{L}^d, \tag{9}$$

$\mathcal{L}^d$ being the Lebesgue measure in $\mathbb{R}^d$. By plugging this representation into Equation (4) we see that the transport velocity (3):

$$\begin{aligned} v_t(x) = v_{\mathrm{d}}(x) &+ \theta \sum_{j=1}^{N} K(x, x_j)\eta_{\mathcal{S}(x)}(x_j) \\ &+ (1-\theta) \int_{\mathbb{R}^d} K(x, y)\eta_{\mathcal{S}(x)}(y)\rho_t(y)\, dy \end{aligned} \tag{10}$$

depends now on a weighted contribution of discrete and continuous dynamics. Clearly, the two choices discussed above correspond to the particular cases $\theta = 0$ (continuous dynamics) and $\theta = 1$ (discrete dynamics). Nevertheless, if $0 < \theta < 1$ this formalism allows one to deal, more in general, with hybrid dynamics which are neither fully discrete nor fully continuous (cf. the case studies presented in Figures 3, 4). Moreover, the transport of the measure (9) by means of Equation (1) with the velocity field (10) allows also for a purely continuous representation of the crowd distribution evolving according to genuinely discrete dynamics or, conversely, a purely discrete representation evolving according to genuinely continuous dynamics. Finally, if the perception parameter θ changes in space, i.e., it is converted into a function of x, then the model enables one to have different types of dynamics in different sub-domains (see e.g., Cristiani et al. (2012), where this idea is used in the case of vehicular traffic for coupling continuous dynamics along straight roads and discrete dynamics at crossroads, where driver perception is sharpened by vehicles coming from different merging directions).

4 Basic theory

Once an initial measure, say $\bar{\mu}$, is prescribed, the model based on Equation (1) together with a velocity field of the type (3)-(4) generates a Cauchy

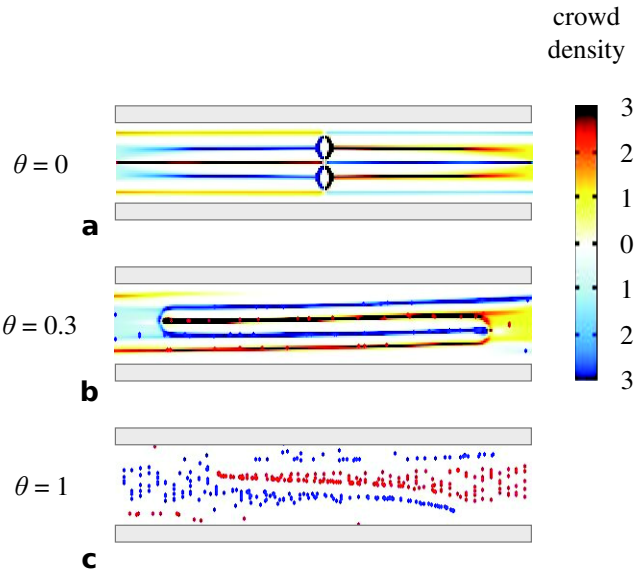

Figure 3. *Lane formation* in counter-flows obtained with model (1)-(3)-(4)-(9) with three different values of the perception parameter θ. **a.** With $\theta = 0$ pedestrian perception is purely *continuous*. Lanes emerge but the lack of *symmetry breaking* makes the result look rather artificial, thereby suggesting that granularity should play a role. **b.** With $\theta = 0.3$ pedestrian perception is genuinely *multiscale*. The atoms of μ_t introduce inhomogeneities in the density flow, which induce a qualitatively more realistic lane formation also at a purely continuous level (i.e., when looking at the density only). **c.** With $\theta = 1$ pedestrian perception is purely *discrete*. Also in this case lane-type patterns predicted by the model look realistic. On the whole, this example demonstrates that lane formation is quite a robust phenomenon at all scales, although pedestrian perception can influence the qualitative patterns collectively observed.

problem falling in the following class:

$$\begin{cases} \dfrac{\partial \mu_t}{\partial t} + \nabla \cdot (\mu_t v[\mu_t]) = 0 \quad x \in \mathbb{R}^d,\ t \in (0, T_{\max}] \\ \mu_0 = \bar{\mu}, \end{cases} \tag{11}$$

where we denoted by $v[\mu_t]$ a generic velocity field fully determined by the (unknown) measure μ_t.

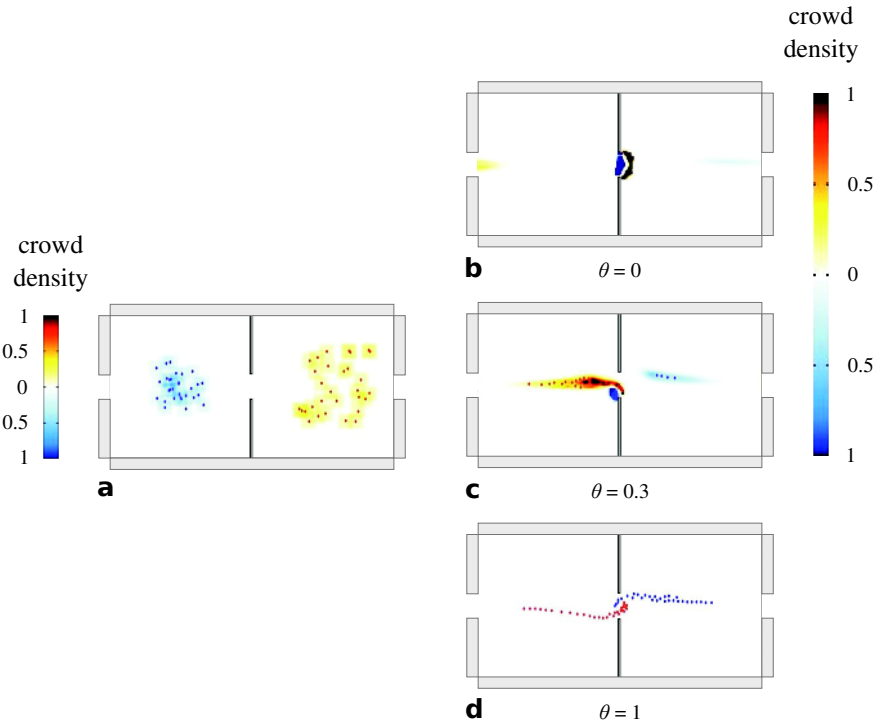

Figure 4. *Crossing flows at a bottleneck* obtained with model (1)-(3)-(4)-(9) with the same three values of the perception parameter θ as in Figure 3. **a.** Initial condition common to all cases. **b.** A purely *continuous* perception ($\theta = 0$) determines a *clogging* of the bottleneck, because individuals interact with subgroups of surrounding walkers being thus basically unable to exploit inter-pedestrian gaps. **c.** A genuinely *multiscale* perception (here with $\theta = 0.3$) produces instead a kind of *traffic light effect* at the bottleneck: the latter is occupied alternately by either crowd while the other one stops and waits. **d.** A purely *discrete* perception ($\theta = 1$) gives rise to an ordered *lane formation* through the bottleneck, for pedestrians estimate with great precision the position of nearby people and self-organize so as to share effectively the available room. On the whole, this example demonstrates that pedestrian perception can play a major role in shaping the observable collective patterns even starting from the very same initial conditions. Notice that all patterns shown in **b.**, **c.**, and **d.** can actually happen in real situations.

In general μ_t is a finite measure on $\mathbb{R}^d$ but not a probability measure. In fact we know that if $\bar{\mu}(\mathbb{R}^d) = N$ then $\mu_t(\mathbb{R}^d) = N$ for all $t \leq T_{\max}$ but clearly it has to be $N > 1$ in order for the model to describe interesting scenarios. However, for the analytical study of Problem (11) it is convenient to rescale μ_t with respect to the total number N of pedestrians in such a way that it is formally a probability, regardless of its derivation for modeling purposes. This way it is easier to set Problem (11) in the proper functional spaces with the proper metrics. Therefore we will henceforth assume to have implicitly performed such a rescaling (and we still denote by μ_t the rescaled measure)[1].

A proper weak sense in which Problem (11) can be understood is the one specified in (2) (with $\mu_0 = \bar{\mu}$). In particular, Equation (2) is well-defined if $t \mapsto \mu_t$ is a continuous mapping from the interval $(0, T_{\max}]$ into one of the metric spaces $\mathcal{P}_p(\mathbb{R}^d)$ of probability measures on $\mathbb{R}^d$ with finite p-th moment ($p \geq 1$, see Ambrosio et al. (2008) for technical details). Without loss of generality we fix $p = 1$, i.e., we consider the space $\mathcal{P}_1(\mathbb{R}^d)$, which is complete with the metric

$$W_1(\mu, \nu) = \sup_{\varphi \in \mathrm{Lip}_1(\mathbb{R}^d)} \int_{\mathbb{R}^d} \varphi \, d(\nu - \mu) \qquad (\mu, \nu \in \mathcal{P}_1(\mathbb{R}^d)),$$

called the *(first) Wasserstein distance*. In the definition above, $\mathrm{Lip}_1(\mathbb{R}^d)$ is the set of Lipschitz continuous functions on $\mathbb{R}^d$ whose Lipschitz constant is not greater than 1.

Ultimately, we say that:

Definition 4.1. A curve $\mu_\bullet \in C([0, T_{\max}]; \mathcal{P}_1(\mathbb{R}^d))$ is a (weak) solution to Problem (11) if it satisfies Equation (2), with $\mu_0 = \bar{\mu}$, for all $\phi \in C_c^\infty(\mathbb{R}^d)$ and all $t \in (0, T_{\max}]$.

The basic theory for Problem (11) depends essentially on the properties of the velocity field. We now formulate some assumptions, valid for sufficiently general fields v (i.e., not necessarily referred to the specific structure (3)-(4)), whence both the well-posedness of the Cauchy problem and the convergence of a suitable numerical scheme, based on the transport of measures, for the approximation of the solutions follow.

[1] Notice that if μ_t is thought of as a probability measure then the interaction velocity (4) must be coherently rewritten as

$$v_{\mathrm{i}}[\mu_t](x) = N \int_{\mathbb{R}^d} K(x, y) \eta_{\mathcal{S}(x)}(y) \, d\mu_t(y)$$

in view of the rescaling.

Assumptions on the velocity v for Problem (11)

(i) *Uniform boundedness*: there exists a constant $V_{\max} > 0$ such that

$$|v[\mu](x)| \leq V_{\max}, \qquad \forall\, x \in \mathbb{R}^d,\ \forall\, \mu \in \mathcal{P}_1(\mathbb{R}^d).$$

(ii) *Lipschitz continuity*: there exists a constant $\mathrm{Lip}(v) > 0$ such that

$$|v[\nu](y) - v[\mu](x)| \leq \mathrm{Lip}(v)\,(|y - x| + W_1(\mu,\, \nu))\,,$$

$\forall\, x,\, y \in \mathbb{R}^d$, $\forall\, \mu,\, \nu \in \mathcal{P}_1(\mathbb{R}^d)$.

(iii) *Mild linearity*: for all $\alpha \in [0,\, 1]$ and all pairs of measures $\mu,\, \nu \in \mathcal{P}_1(\mathbb{R}^d)$ it results

$$v[\alpha\mu + (1 - \alpha)\nu] = \alpha v[\mu] + (1 - \alpha)v[\nu].$$

Remark 4.2. We called Assumption (iii) *mild linearity* because it requires the mapping $\mu \mapsto v[\mu]$ to be linear for *convex* linear combinations only.

It is important to take into account that the Assumptions above are not meant to be sharp from the technical point of view. Rather, they are thought of for models which should be applied to realistic case studies. In this respect, one of their advantages is that they can be verified quite easily in practical cases. Furthermore, they allow for proofs which do not require sophisticated techniques of optimal transportation.

4.1 Well-posedness of Problem (11)

Using only Assumption (ii) it is possible to prove the following *a priori* estimate on the solutions to Problem (11):

Theorem 4.3. *If $\mu^1_\bullet,\, \mu^2_\bullet \in C([0,\, T_{\max}];\, \mathcal{P}_1(\mathbb{R}^d))$ are two solutions corresponding to two initial data $\bar\mu^1,\, \bar\mu^2 \in \mathcal{P}_1(\mathbb{R}^d)$, respectively, then there exists a constant $\mathcal{C} > 0$ such that*

$$W_1(\mu^1_t,\, \mu^2_t) \leq \mathcal{C} W_1(\bar\mu^1,\, \bar\mu^2), \qquad \forall\, t \in (0,\, T_{\max}]. \tag{12}$$

Proof. See e.g., Cristiani et al.. □

Thus the solution to Problem (11), if it exists, is unique and depends continuously on the initial datum. The constant $\mathcal{C}$ depends on the Lipschitz constant $\mathrm{Lip}(v)$ of the velocity and on the final time $T_{\max}$.

For the proof of the estimate (12) the interested reader is referred to the above-cited reference. Here we simply point out that the classical technique makes use of the following *representation formula* of the solutions to Problem (11): if $\mu_\bullet \in C([0, T_{\max}]; \mathcal{P}_1(\mathbb{R}^d))$ is a solution corresponding to an initial datum $\bar{\mu} \in \mathcal{P}_1(\mathbb{R}^d)$ then, after introducing the *flow map* $\gamma_t : \mathbb{R}^d \to \mathbb{R}^d$ defined by:

$$\begin{cases} \dfrac{\partial}{\partial t}\gamma_t(x) = v[\mu_t](\gamma_t(x)), & x \in \mathbb{R}^d,\ t \in (0, T_{\max}] \\ \gamma_0(x) = x, & x \in \mathbb{R}^d, \end{cases} \tag{13}$$

it results

$$\mu_t = \gamma_t \# \bar{\mu} \quad \text{viz.} \quad \mu_t(E) = \bar{\mu}(\gamma_t^{-1}(E)),\ \forall\, E \in \mathcal{B}(\mathbb{R}^d),$$

where $\#$ is the so-called *push forward* operator. This representation formula can be easily checked using Equation (2).

Next, in view of the further Assumptions (i), (iii), also existence of the solution can be proved:

Theorem 4.4. *For $\bar{\mu} \in \mathcal{P}_2(\mathbb{R}^d) \subset \mathcal{P}_1(\mathbb{R}^d)$ there exists a solution $\mu_\bullet \in C([0, T_{\max}]; \mathcal{P}_1(\mathbb{R}^d))$ to Problem* (11).

Proof. See e.g., Tosin and Frasca (2011). □

Notice that Theorem 4.4 requires actually $\bar{\mu} \in \mathcal{P}_2(\mathbb{R}^d)$, i.e., that the initial datum has both first and second order moments finite. This assumption is mainly technical. Nevertheless, from the point of view of applications it is not a limitation, since initial data typically have *compact* support (indeed, a crowd spread over the whole $\mathbb{R}^d$ would not be such a realistic initial condition), hence their moments of *any* order p are automatically finite. In fact:

$$\int_{\mathbb{R}^d} |x|^p \, d\bar{\mu}(x) = \int_{\mathrm{supp}(\bar{\mu})} |x|^p \, d\bar{\mu}(x) \leq R^p < +\infty,$$

R being the radius of one of the balls centered at the origin which contain $\mathrm{supp}(\bar{\mu})$.

Finally, we can establish the following well-posedness result, in the sense of Hadamard, for the Cauchy problem (11):

Theorem 4.5. *Let Assumptions (i)–(iii) hold. For all* $\bar{\mu} \in \mathcal{P}_2(\mathbb{R}^d)$ *there exists a unique solution* $\mu_\bullet \in C([0, T_{\max}]; \mathcal{P}_1(\mathbb{R}^d))$ *to Problem* (11) *in the sense of Definition 4.1. In addition, it depends continuously on the initial datum on the basis of the estimate* (12).

4.2 Numerical scheme and its convergence

In order to approximate the solution to Problem (11) it is possible to use the numerical scheme introduced by Piccoli and Tosin (2009, 2011), then further detailed for multiscale models by Cristiani et al. (2011) and adopted also by Maury et al. (2010); Canuto et al. (2012). In short, the idea is to approximate μ_t by an *absolutely continuous* measure with respect to Lebesgue, which is piecewise constant over a pairwise disjoint partition of $\mathbb{R}^d$ called *mesh*. Specifically, the latter is formed by cells E_i of characteristic size $h > 0$ such that $\mathcal{L}^d(E_i) \to 0$ when $h \to 0^+$:

$$\mathbb{R}^d = \bigcup_{i \in \mathbb{Z}^d} E_i, \qquad E_i \cap E_j = \emptyset \quad \forall\, i \neq j.$$

For $d = 2$ (which in several applications is the most interesting case for crowd simulations) the cells E_i can be square-shaped with edge length h. The simplest generalization to an arbitrary dimension is obtained by considering hypercubes with edge length h, so that $\mathcal{L}^d(E_i) = h^d$.

Let $\tilde{\mu}_n$ be the approximation of μ_t at the discrete time $t_n = n\Delta t$, where $\Delta t > 0$ is a fixed time step. Then by construction it results $d\tilde{\mu}_n = \tilde{\rho}_n\, dx$, where $\tilde{\rho}_n = \tilde{\rho}_n(x) : \mathbb{R}^d \to \mathbb{R}_+$ is the density that the numerical scheme has to determine. Again by construction, $\tilde{\rho}_n$ is piecewise constant on the grid $\{E_i\}_{i \in \mathbb{Z}^d}$, therefore it can be represented as

$$\tilde{\rho}_n(x) = \sum_{i \in \mathbb{Z}^d} \rho_i^n \chi_{E_i}(x), \tag{14}$$

χ_{E_i} denoting the characteristic function of the cell E_i. The unknowns are thus the coefficients $\rho_i^n \geq 0$.

The numerical scheme is constructed by imposing first that, in one time step, the measure $\tilde{\mu}_n$ is transported on the new measure $\tilde{\mu}_{n+1}$ by a suitable discretization $\tilde{\gamma}_n$ of the flow map (13): $\tilde{\mu}_{n+1} = \tilde{\gamma}_n \# \tilde{\mu}_n$, and by testing then this relation on the grid cells: $\tilde{\mu}_{n+1}(E_i) = \tilde{\mu}_n(\tilde{\gamma}_n^{-1}(E_i))$. Using the numerical density (14), this yields a recursive formula to pass from the coefficients ρ_i^n to those at the next time step:

$$\rho_i^{n+1} = \frac{1}{h^d} \sum_{j \in \mathbb{Z}^d} \rho_j^n \mathcal{L}^d(E_i \cap \tilde{\gamma}_n(E_j)) \quad (i \in \mathbb{Z}^d). \tag{15}$$

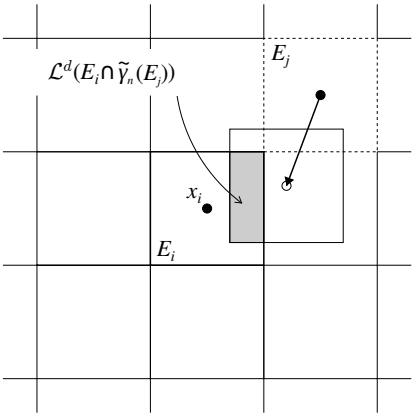

Figure 5. Action of the numerical scheme (15) on the grid cells.

It expresses the fact that the numerical density is redistributed over the mesh, in one time step, proportionally to the (Lebesgue) measure of the intersections among the cells moved by the discrete flow map $\tilde{\gamma}_n$ (see Figure 5). In particular, the latter is obtained cell-by-cell as:

$$\tilde{\gamma}_n(x) = x + v[\tilde{\mu}_n](x_i)\Delta t \quad \text{for } x \in E_i,$$

where x_i is any point of E_i, for instance its center. Hence $\tilde{\gamma}_n$ acts in every cell as a rigid translation with constant velocity $v[\tilde{\mu}_n](x_i)$, namely the velocity v of the exact problem (11) computed for $x = x_i$ with respect to the approximate measure $\tilde{\mu}_n$.

Despite that the numerical measure $\tilde{\mu}_n$ has been chosen absolutely continuous with respect to Lebesgue, the scheme (15) can actually approximate solutions to Problem (11) with generic spatial structure. Indeed the following result holds true:

Theorem 4.6. *Consider a sequence of spatiotemporal grids indexed by* $k = 0, 1, 2 \ldots$, *with mesh parameters* $h_k, \Delta t_k \to 0$ *for* $k \to \infty$. *Let* $\tilde{\mu}_t^k$ *be the piecewise linear interpolation in time of the numerical solutions* $\tilde{\mu}_n^k$ *computed on the* k*-th mesh with the scheme* (15)*:*

$$\tilde{\mu}_t^k = \sum_{n=0}^{N_{\max}^k - 1} \left[\left(1 - \frac{t - t_n^k}{\Delta t_k} \right) \tilde{\mu}_n^k + \frac{t - t_n^k}{\Delta t_k} \tilde{\mu}_{n+1}^k \right] \chi_{[t_n^k,\, t_{n+1}^k]}(t), \qquad (16)$$

where $t_n^k = n\Delta t_k$, $N_{\max}^k$ *is the number of discrete time steps on the* k*-th grid needed to reach the final time* $T_{\max}$*, and* $\chi_{[t_n^k,\, t_{n+1}^k]}$ *denotes the characteristic function of the interval* $[t_n^k,\, t_{n+1}^k]$.

Assume that Assumptions (i)–(iii) on page 12 hold true, that the initial datum is discretized as:

$$(\rho_i^0)^k = \frac{\bar\mu(E_i^k)}{h_k^d} \quad (i \in \mathbb{Z}^d),$$

and moreover that the spatiotemporal grids are chosen in such a way that

$$h_k = o(\Delta t_k) \quad \textit{when} \quad k \to \infty.$$

If $\tilde\mu_\bullet^k$ *converges in* $C([0,\, T_{\max}];\, \mathcal{P}_1(\mathbb{R}^d))$ *to some* $\mu_\bullet$ *for* $k \to \infty$ *in the following sense:*

$$\lim_{k\to\infty} \sup_{t\in[0,\, T_{\max}]} W_1(\tilde\mu_t^k,\, \mu_t) = 0$$

then the limit $\mu_\bullet$ *is a (weak) solution to Problem* (11) *in the sense of Definition 4.1.*

Proof. See e.g., Tosin and Frasca (2011). □

Notice that Theorem 4.6 does not guarantee but *assumes* the convergence of the numerical solution to a curve $\mu_\bullet \in C([0,\, T_{\max}];\, \mathcal{P}_1(\mathbb{R}^d))$. For this reason, it recalls the Lax-Wendroff's Theorem about the convergence of numerical schemes for hyperbolic conservation laws. Nevertheless it is possible to complement it with a simple criterion ensuring that the required convergence does indeed take place:

Proposition 4.7. *Let a compact set* $K \subset \mathbb{R}^d$ *exist such that* $\operatorname{supp}(\tilde\mu_n^k) \subseteq K$ *for all* n *and all* k*. Then the time-interpolated sequence* $\{\tilde\mu_\bullet^k\}_{k\geq 0}$*, cf. Equation* (16)*, converges in* $C([0,\, T_{\max}];\, \mathcal{P}_1(\mathbb{R}^d))$.

Proof. See e.g., Tosin and Frasca (2011). □

It is evident that such a K exists especially when the initial datum $\bar\mu$ is compactly supported. In fact, due to Assumption (i), Problem (11) describes a transport with *finite* speed, hence $\operatorname{supp}(\bar\mu)$ cannot expand indefinitely within a finite time $T_{\max}$.

Besides the references already given for the proofs of Theorem 4.6 and of Proposition 4.7, the interested reader is referred also to the paper by Piccoli and Rossi (2013) for a deep analysis of further numerical schemes dealing with the approximation of the solution to Problem (11).

4.3 Structure of the solution

The theory set forth in the previous sections does not provide any information about the spatial structure of the solutions to Problem (11), which is important especially for multiscale models discussed in Section 3.

Using the representation formula introduced in Section 4.1, it is quite easy to see that if the initial datum $\bar{\mu}$ has a discrete structure like[2] $\bar{\mu} = \frac{1}{N}\sum_{i=1}^{N}\delta_{\bar{x}_i}$ then also the solution μ_t has a discrete structure for all $t > 0$. In fact, for all Borel set $E \in \mathcal{B}(\mathbb{R}^d)$ it results:

$$\mu_t(E) = (\gamma_t \# \bar{\mu})(E) = \bar{\mu}(\gamma_t^{-1}(E)) = \frac{1}{N}\sum_{i=1}^{N}\delta_{\bar{x}_i}(\gamma_t^{-1}(E)) = \frac{1}{N}\sum_{i=1}^{N}\delta_{\gamma_t(\bar{x}_i)}(E),$$

hence letting $x_i(t) := \gamma_t(\bar{x}_i)$ we have $\mu_t = \frac{1}{N}\sum_{i=1}^{N}\delta_{x_i(t)}$. Notice that this holds independently of the regularity of the flow map γ_t, namely of the velocity field $v[\mu_t]$.

Conversely, for an absolutely continuous initial datum, $d\bar{\mu}(x) = \bar{\rho}(x)\,dx$, the solution μ_t may develop singularities in finite time if the flow map tends to concentrate "too much" density over "too small" spatial structures. The following result gives a sufficient condition for ruling out this possibility:

Theorem 4.8. *Let $\bar{\mu}$ be absolutely continuous with respect to the Lebesgue measure. Assume that at every fixed time $t \in (0, T_{\max}]$ there exists a constant $\mathcal{C}_t > 0$, possibly depending on t, such that*

$$\mathcal{L}^d(\gamma_t^{-1}(E)) \le \mathcal{C}_t \mathcal{L}^d(E), \qquad \forall\, E \in \mathcal{B}(\mathbb{R}^d). \tag{17}$$

Then also $\mu_t = \gamma_t \# \bar{\mu}$ is absolutely continuous with respect to Lebesgue for all $t \in (0, T_{\max}]$.

Proof. See e.g., Cristiani et al. (2011); Piccoli and Tosin (2011); Cristiani et al.. □

Condition (17) requires that the flow map does not shrink measurable sets too much. Indeed, by reading the inequality from right to left, it states that the Lebesgue measure of E can be controlled *from below* by the measure of its inverse image through γ_t. Nevertheless, this condition is not easy to be checked in concrete cases. To obviate such a difficulty, at least for smooth flow maps, it is possible to use the following criterion, which is at the same time sufficient and easier to verify.

[2] Unlike Equation (5), here the coefficient $\frac{1}{N}$ appears because of the rescaling to a probability measure introduced at the beginning of the section.

Proposition 4.9. *If the flow map γ_t is a diffeomorphism with Lipschitz constant* $\mathrm{Lip}(\gamma_t)$ *such that*

$$\mathrm{Lip}(\gamma_t) < \frac{1}{\mathrm{Lip}(v)T_{\max}} \tag{18}$$

then it fulfills condition (17)*.*

Proof. See e.g., Cristiani et al.. □

In particular, it is useful to know that under Assumption (ii) the Lipschitz constant of γ_t can be estimated as $\mathrm{Lip}(\gamma_t) \leq 1 + \mathrm{Lip}(v)T_{\max}e^{\mathrm{Lip}(v)T_{\max}}$ (see Cristiani et al.), hence (18) is certainly satisfied if

$$1 + \mathrm{Lip}(v)T_{\max}e^{\mathrm{Lip}(v)T_{\max}} < \frac{1}{\mathrm{Lip}(v)T_{\max}},$$

which is ultimately a condition on the Lipschitz constant of the velocity. This is more practical because, as seen in Section 2.1, it is the velocity, not the flow map, which plays a major role in the modeling approach.

Finally, if the initial datum has a hybrid structure such as (9) it is sufficient to recall the linearity of the push forward operator # to conclude that the results above apply separately to the discrete and continuous parts. Consequently, if the flow map satisfies the conditions expressed by Theorem 4.8 and by Proposition 4.9 then the solution to Problem (11) preserves the multiscale structure for all times $t > 0$.

5 Back to crowd models

Results presented in Section 4 hold for an "abstract" velocity field characterized essentially by Assumptions (i)–(iii) (cf. page 12). In order to construct crowd models not only physically realistic but also mathematically robust it is therefore important to study the interplay between the structures introduced in Section 2 and these assumptions.

As recalled in Section 2.1, the interaction kernel K should depend on the *relative position* $y - x$ of the interacting pedestrians in order for the description of the interactions to be independent of rigid transformations of the coordinate system. This implies

$$K(x, y) = k(y - x),$$

$k : \mathbb{R}^d \to \mathbb{R}^d$ being a function to be properly modeled (which we still call *interaction kernel*). That said, pedestrian velocity (3)-(4) takes the form:

$$v[\mu_t](x) = v_{\mathrm{d}}(x) + N \int_{\mathbb{R}^d} k(y - x)\eta_{\mathcal{S}(x)}(y)\, d\mu_t(t), \tag{19}$$

where the coefficient N (total number of pedestrians) in front of the interaction integral appears because of the reinterpretation of μ_t as a probability measure (cf. footnote 1 on page 11).

It is immediate to check that the velocity field (19) satisfies Assumption (iii) with no additional hypotheses. In fact, it is sufficient to write $v_{\mathrm{d}} = \alpha v_{\mathrm{d}} + (1-\alpha)v_{\mathrm{d}}$ and to collect the terms conveniently. Notice that it is fundamental that Assumption (iii) requires only a *mild* linearity, for the mapping $\mu \mapsto v[\mu]$ resulting from Equation (19) is in general not linear (except when the desired velocity is zero, which however does not always make sense from the modeling point of view).

In order for the velocity (19) to fulfill also Assumptions (i), (ii) some further technical details are needed, to be regarded as modeling guidelines, concerning the structure of the terms v_{d}, k, $\mathcal{S}(\cdot)$, and $\eta_{\mathcal{S}(\cdot)}$. For the sake of simplicity we consider only the two-dimensional case ($d = 2$), which is however largely sufficient for addressing realistic crowd models.

Modeling Guidelines for the velocity v (19) with $d = 2$

(i) *Desired velocity*: let $x \mapsto v_{\mathrm{d}}(x)$ be Lipschitz continuous and bounded in $\mathbb{R}^2$.

(ii) *Sensory region*: for all $x \in \mathbb{R}^2$, let $\mathcal{S}(x)$ be a bounded Borel set contained in a ball with fixed radius $R > 0$ independent of x (for instance, the one centered in x: $\mathcal{S}(x) \subseteq B_R(x)$) and isometric to a reference set $\mathcal{S}(0) \subseteq B_R(0)$.

(iii) *Interaction kernel*: let $x \mapsto k(x)$ be Lipschitz continuous in the ball $B_R(0)$ centered at the origin and with radius R defined at the previous point (ii).

(iv) *Cut-off function*: for all $E \in \mathcal{B}(\mathbb{R}^2)$, let $x \mapsto \eta_E(x)$ be Lipschitz continuous and bounded between 0 and 1 in $\mathbb{R}^2$ with $\mathrm{supp}(\eta_E) \subset\subset E$.

Remark 5.1. The Modeling Guideline (ii) means that the sensory region $\mathcal{S}(x)$ of the point x is obtained by translating and rotating the reference set $\mathcal{S}(0)$. The translation vector is obviously x. Moreover, according to what has been said in Section 2.1, the rotation angle is individuated by the direction of the vector $v_{\mathrm{d}}(x)$.

If pedestrian velocity is constructed in accordance with the Modeling Guidelines stated above then the crowd model based on Equations (1), (19) features a certain mathematical robustness, indeed:

Proposition 5.2. *If, in two space dimensions ($d = 2$), the velocity field* (19) *complies with the Modeling Guidelines (i)–(iv) then it fulfills Assumptions (i)–(iii).*

Proof. See e.g., Tosin and Frasca (2011). □

hence it is possible to apply to it the theory of well-posedness and numerical approximation presented in Section 4.

Bibliography

L. Ambrosio, N. Gigli, and G. Savaré. *Gradient flows in metric spaces and in the space of probability measures*. Lectures in Mathematics ETH Zürich. Birkhäuser Verlag, Basel, second edition, 2008.

L. Bruno, A. Tosin, P. Tricerri, and F. Venuti. Non-local first-order modelling of crowd dynamics: A multidimensional framework with applications. *Appl. Math. Model.*, 35(1):426–445, 2011.

C. Canuto, F. Fagnani, and P. Tilli. An Eulerian approach to the analysis of Krause's consensus models. *SIAM J. Control Optim.*, 50(1):243–265, 2012.

R. M. Colombo and M. D. Rosini. Existence of nonclassical solutions in a pedestrian flow model. *Nonlinear Anal. Real World Appl.*, 10(5):2716–2728, 2009.

V. Coscia and C. Canavesio. First-order macroscopic modelling of human crowd dynamics. *Math. Models Methods Appl. Sci.*, 18(1 suppl.):1217–1247, 2008.

E. Cristiani, B. Piccoli, and A. Tosin. Multiscale Modeling of Pedestrian Dynamics. In preparation.

E. Cristiani, B. Piccoli, and A. Tosin. Modeling self-organization in pedestrians and animal groups from macroscopic and microscopic viewpoints. In G. Naldi, L. Pareschi, and G. Toscani, editors, *Mathematical Modeling of Collective Behavior in Socio-Economic and Life Sciences*, Modeling and Simulation in Science, Engineering and Technology, pages 337–364. Birkhäuser, Boston, 2010.

E. Cristiani, B. Piccoli, and A. Tosin. Multiscale modeling of granular flows with application to crowd dynamics. *Multiscale Model. Simul.*, 9 (1):155–182, 2011.

E. Cristiani, B. Piccoli, and A. Tosin. How can macroscopic models reveal self-organization in traffic flow? In *Proceedings of the 51st IEEE Conference on Decision and Control*, Maui, Hawaii, USA, December 2012.

B. Maury, A. Roudneff-Chupin, and F. Santambrogio. A macroscopic crowd motion model of gradient flow type. *Math. Models Methods Appl. Sci.*, 20(10):1787–1821, 2010.

B. Piccoli and F. Rossi. Transport equation with nonlocal velocity in Wasserstein spaces: convergence of numerical schemes. *Acta Appl. Math.*, 124(1):73–105, 2013.

B. Piccoli and A. Tosin. Pedestrian flows in bounded domains with obstacles. *Contin. Mech. Thermodyn.*, 21(2):85–107, 2009.

B. Piccoli and A. Tosin. Time-evolving measures and macroscopic modeling of pedestrian flow. *Arch. Ration. Mech. Anal.*, 199(3):707–738, 2011.

E. Schröedinger. *What is Life? Mind and Matter*. Cambridge University Press, 1967.

A. Tosin and P. Frasca. Existence and approximation of probability measure solutions to models of collective behaviors. *Netw. Heterog. Media*, 6(3): 561–596, 2011.